Reconfigurable RF Filter Based on Cascaded Microring Resonators

Ziyang Lu, Jiachen Li, Yunhao Wu, Hongwei Chen, *Senior Member, IEEE*, Sigang Yang, and Minghua Chen

***Abstract*—To meet the requirement of radio frequency signal processing tasks among various frequency bands, here we have demonstrated a reconfigurable microwave photonic bandpass filter by flipping the optical notch spectrum of a cascaded microring resonator (MRR) filter pool chip through phase modulation. We experimentally characterize the cascaded MRR filter pool chip on the Si3N4 platform and evaluate the system performance of the established microwave photonic filter (MPF). In the demonstrated microwave photonic filter system, the center frequency can be tuned within 5.8–18.2 GHz and the bandwidth can be tuned within 2.1–3.5 GHz. In particular, the MPF system features a response with a shape factor of ∼2.2. With the advantages of reconfigurability and good shape factor, the demonstrated reconfigurable RF bandpass filter shows a potential application in future software-defined RF frontends.**

***Index Terms*—Microwave photonic filter, reconfigurability.**

I. Introduction

RADIO frequency (RF) frontends with broad operation bandwidth are of growingly need for processing numerous signal processing tasks over various frequency bands, such as satellite communication systems [1], arrayed radar signal receivers [2], and electronic warfare [3]. Recently, software-defined RF frontends [4], [5] with high flexibility and tunability are preferred due to their reconfigurability for complicate and dynamic environments. To realize the tunable RF frontend, reconfigurable RF bandpass filters are required, which select the expected operation frequency band [6]. However, achieving wide operation bandwidth is hard for traditional microwave devices, and their frequency range is typically restricted to several gigahertz [7], [8]. Therefore, it is challenging for electronic methods to construct reconfigurable RF bandpass filters operating over large frequency range.

Microwave photonic technologies, with various advantages of wide operation bandwidth, significant reconfigurability and immunity to electromagnetic interference [9], [10], [11], provide a potential method to overcome the limitations of RF filters in tunability. Furthermore, the response of bandpass MPF is preferred to have good shape factor, which can increase the frequency selectivity and the out-of-band suppression [12].

Numerous studies have been conducted on reconfigurable bandpass MPFs, which can be broadly divided into two types. The first one is directly mapping the response of a single optical bandpass filter to the RF domain. In this method, the reconfigurability and the shape factor (defined as the ratio of bandwidth at 20 dB to 3 dB) of the MPF are decided by the employed optical bandpass filter. Typical schemes of the required reconfigurable rectangular optical filters include series microring resonators (MRRs) [13], [14], [15], [16], ring-assisted Mach-Zehnder interferometer (RAMZI) [17], [18], [19] and optical lattice filter [20], [21], all of them face the problem of complicated structure and high optical loss. In the second type, the response of the RF bandpass filter is obtained by flipping that of optical notch filter with the help of the phase modulation. This method can realize a compact MPF with low cost and low consumption [22]. However, the optical notch filters, which are the key components in this method, are lack of bandwidth reconfigurability [23]. A promising structure to solve this problem in the second type is cascaded MRR filter pool [24], [25]. Cascaded MRR filter pool is composed of several independent MRR notch filters, of which the responses can be combined to construct a notch spectrum with good shape factor. Moreover, this combined optical notch spectrum is flipped to obtain a RF bandpass response with the second MPF system. This proposed optical notch filter also features much less optical loss and simpler structure [26], compared with the employed optical rectangular bandpass filter in the first type. Besides, since the optical loss of the pool is barely irrelevant to the number of cascaded MRRs, this scheme shows a potential for further extension to improve the reconfigurability. Another way to realize MPF system with cascaded MRR notch filters is to introduce π phase shift with over coupling MRRs in dual sidebands after phase modulation [27], [28]. The phase difference in two sidebands brings a RF passband after photodetection. This scheme provides great reconfigurability and low optical loss, but the ripple in passband might be large in part of those works. A multiband MPF is also realized in this way with a single MRR [29], which exhibits simple structure and great bandwidth reconfigurability, but the rejection ratio needs improve. Except of the methods stated above, alternative solutions for the reconfigurable bandpass MPF, such like stimulated Brillouin scattering (SBS) [30], are difficult to be integrated, and the control of them is complex.

Manuscript received 28 February 2023; revised 3 April 2023; accepted 16 May 2023. Date of publication 19 May 2023; date of current version 30 May 2023. *(Corresponding author: Minghua Chen.)*

Ziyang Lu and Yunhao Wu are with the Tsinghua University, Beijing 100084, China (e-mail: lu-zy19@mails.tsinghua.edu.cn; panwoo_wuyh@126.com).

Jiachen Li, Hongwei Chen, Sigang Yang, and Minghua Chen are with the Department of Electronic Engineering, Tsinghua University, Beijing 100084, China (e-mail: lijc17@mails.tsinghua.edu.cn; chenhw@tsinghua.edu.cn; ysg@tsinghua.edu.cn; chenmh@tsinghua.edu.cn).

Digital Object Identifier 10.1109/JPHOT.2023.3278052

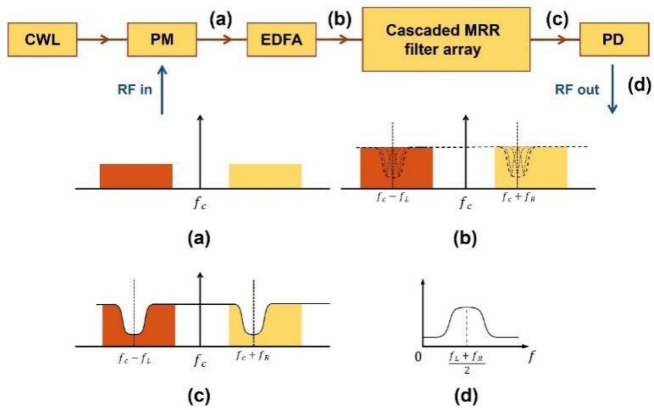

Fig. 1. Schematic of the reconfigurable bandpass MPF. (a) Optical spectrum of the phase modulation signal. (b) The phase modulation signal after the EDFA. (c) Optical spectrum of the phase modulation signal after filtering. (d) The RF response of the MPF. CWL: Continuous wave laser, PM: phase modulator, EDFA: Erbium-doped fiber amplifier, PD: Photodetector.

In this paper, we report a reconfigurable bandpass MPF with good shape factor, which is constructed with a cascaded MRR filter pool and flipping the notch response of optical notch filter based on the phase modulation. The cascaded MRR filter pool is composed with six MRRs and fabricated on the silicon nitride (Si_3N_4) platform, with a micro-heater deposited on each MRR. By adjusting the voltages on the micro-heaters to change the center frequencies of the MRRs, and thus control the spectrum of the notch filter pool, we realize a reconfigurable bandpass MPF with tunable center frequency from 5.8 GHz to 18.2 GHz. The bandwidth can also be reconfigured within 2.1–3.5 GHz. This MPF exhibits a filter response with a shape factor of ∼2.2 despite the change of the center frequency and the bandwidth. Besides, the passband ripples are limited under 2.5 dB. Furthermore, this work provides a robust framework where the number of cascaded MRRs can be arbitrarily extended due to the low optical loss of this notch filter pool. The demonstrated reconfigurable bandpass MPF may help in future establishment of satellite communication systems, arrayed radar signal receivers, and electronic warfare.

II. Operation Principle

Fig. 1 shows the structure of the proposed reconfigurable MPF. The input RF signal is introduced to the optical path through a phase modulator (PM) and generates a double sideband signal. Under small signal condition, the phase modulation signal can be described as

$$E_{PM}(t) = \sqrt{P_0}\begin{Bmatrix} J_0(m)\cos(2\pi f_c t) \\ +J_1(m)\cos\left(2\pi(f_c+f_{RF})t+\frac{\pi}{2}\right) \\ -J_1(m)\cos\left(2\pi(f_c-f_{RF})t-\frac{\pi}{2}\right)\end{Bmatrix}, \tag{1}$$

where P_0 is the power of the laser source, J_n $(n = 0, 1)$ is the n-order Bessel function of the first kind, f_c is the carrier frequency, and f_{RF} is the frequency of the input RF signal. The spectrum of the phase modulation signal illustrated by (1) is shown in Fig. 1(a), where the two symmetric sidebands with the same amplitude and a 180° phase difference are located on either side of the carrier. The phase modulation signal is then amplified with an erbium-doped fiber amplifier (EDFA) and processed by the cascaded MRR filter pool. Here, the center frequencies of all the MRRs are designed to be tunable. The optical spectrum of the processed phase modulation signal is displayed in Fig. 1(c). To simply explain the principle, we suppose that the number of cascaded MRRs is 2N. The center frequencies are properly tuned to ensure that each sideband is processed with N MRRs. This symmetry of the number of MRRs can enable nearly full anti-phase cancellation between the two sidebands, and thus increase the rejection ratio and reduce the shape factor of the RF bandpass response [31]. Furthermore, to obtain a single flat RF passband in following steps, the center frequency of the i_{th} ($i = 1, 2, \ldots, 2N$) MRR are required to be described as

$$f_i = \begin{cases} f_c - f_0 - (i-1)\Delta f, & i \in [1,\ N] \\ f_c + f_0 + (i-1)\Delta f, & i \in [N+1,\ 2N] \end{cases}, \tag{2}$$

where f_0 is the distance between carrier frequency and the center frequency of the nearest MRR in frequency domain, and Δf is the separation between the center frequencies of MRRs. (2) describes that the MRRs are combined into two notch filters with the same shape of response and different center frequency $f_c - f_L$ and $f_c + f_R$, as shown in Fig. 1(c). The two sidebands are processed by the combined two notch filters, respectively. In case that the center frequencies are set as (2), f_L and f_R can be expressed as

$$f_L = f_0 + \frac{N-1}{2}\Delta f, \tag{3}$$

$$f_R = f_0 + \frac{3N-1}{2}\Delta f. \tag{4}$$

Afterwards, the signal is fed into the photodetector (PD) and down converted to radio frequency. The variation of the output photocurrent can be expressed as

$$\Delta i_{PD} \propto \begin{Bmatrix} J_0J_1H(f_c)H(f_c+f_{RF})\cos\left(2\pi f_{RF}t+\frac{\pi}{2}\right)+ \\ J_0J_1H(f_c)H(f_c-f_{RF})\cos\left(2\pi f_{RF}t-\frac{\pi}{2}\right)+ \\ J_1^2H(f_c+f_{RF})H(f_c-f_{RF})\cos(4\pi f_{RF}t+\pi)\end{Bmatrix}, \tag{5}$$

In (5), H(f) expresses the notch response of the filter. The terms with frequency beyond RF range are omitted. Consider that $J_0(m) >> J_1(m)$, (5) can be simplified as

$$\Delta i_{PD} \propto (H(f_c+f_{RF}) - H(f_c-f_{RF}))\cos\left(2\pi f_{RF}t+\frac{\pi}{2}\right), \tag{6}$$

or in frequency domain,

$$H_{PD}(f_{RF}) \propto |H(f_c+f_{RF}) - H(f_c-f_{RF})|. \tag{7}$$

Equation (7) reveals that the RF response of the MPF system depends on the combination of the notch filtering spectrum in the two sidebands. Hence the two notch filter spectrums applied on the two sidebands are flipped and combined into a single passband filtering spectrum. As shown in Fig. 1(d), the center

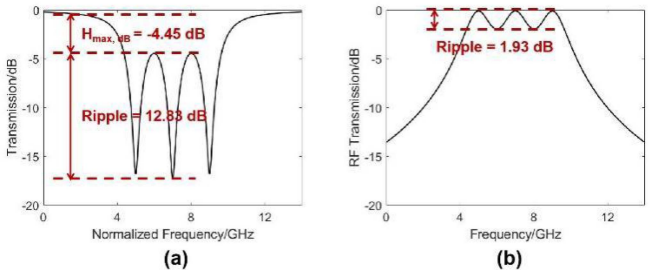

Fig. 2. (a) The theoretical optical transmission spectrum of the cascaded MRR notch filters. The bandwidth of each MRR is 0.8 GHz, and Δf is 2 GHz. (b) The corresponding theoretical RF transmission spectrum. The passband ripple is compressed to 1.93 dB.

frequency of the constructed MPF is decided by f_L and f_R, and the bandwidth depends on Δf. The center frequency can be expressed as

$$f_{MPF} = \frac{f_L + f_R}{2} = f_0 + \frac{2N-1}{2}\Delta f. \tag{8}$$

Since f_L, f_R and Δf in (8) are all tunable through changing the thermal voltages, the RF response exhibits promising reconfigurability. Meanwhile, the combination of several notch filtering spectrums induces good shape factor. Hence, we realize a reconfigurable MPF with small shape factor.

To obtain a flat passband response, Δf is required to be below the 3-dB bandwidth of the MRR to limit the ripple of the notch spectrum. Moreover, the proposed scheme shows great performance in compressing the ripple in the transformation from optical notch spectrum to RF bandpass spectrum. The RF passband ripple could be described as:

$$R_{RF,dB} = 10\log\frac{1-H_{\min}}{1-H_{\max}}. \tag{9}$$

according to (7), where H_{max} and H_{min} are the maximum and minimum transmittance in the stopband of the notch filter, respectively. In case that H_{max} equals to 0.36 and the ripple in notch spectrum is 12.83 dB (i.e., $H_{min} = 0.01$), the RF passband ripple is simulated to be 1.93 dB, as shown in Fig. 2.

We further evaluate the ripple compressing performance by changing the maximum transmittance of the notch spectrum. As shown in Fig. 3, the ripple could be compressed logarithmically from optical notch spectrum to RF bandpass spectrum. This shows a potential for realizing limited passband ripple with proper H_{max} in this scheme.

III. Chip Fabrication and Experimental Results

Fig. 4 displays the experimental construction of the proposed reconfigurable bandpass MPF. A continuous wave laser with 14.2 dBm output power at 1552.28 nm is connected to a PM. The output phase modulation signal is then amplified with an EDFA to compensate the optical loss induced by the PM and reaches 16 dBm power. The amplified phase modulation signal is subsequently coupled into the fabricated cascaded MRR filter pool chip. The chip is demonstrated on the Si_3N_4 waveguide platform, and the fabrication process has been stated in a previous paper [32]. The MRR filter pool are cascaded by six MRRs,

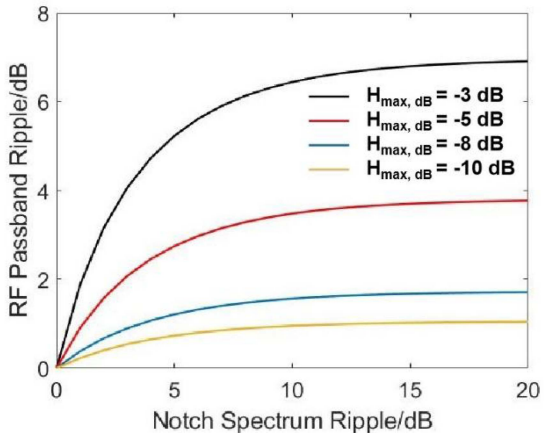

Fig. 3. The relation between RF passband ripple and optical notch spectrum ripple with different H_{max}.

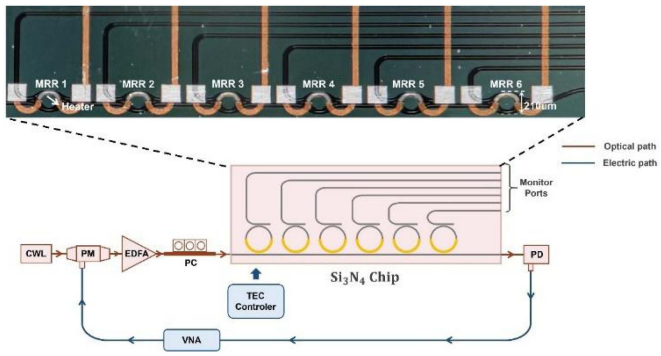

Fig. 4. Experimental construction of the MPF. A micrograph of the fabricated Si_3N_4 chip is also displayed. PC: Polarization controller, TEC: thermo electric cooler, VNA: Vector network analyzer.

occupying an area of 6.5 $\times$ 1.8 mm, as shown in the inset of Fig. 4. Here, the diameter and the coupling gap of all the MRRs are set to be 210 um and 1.1 um, respectively. Besides, microheater is employed on each MRR to control the corresponding center frequency. Furthermore, we place a thermo-electric cooler (TEC) under the Si_3N_4 chip for stabilizing the center frequencies of this filter pool in fluctuating environmental conditions. The optical coupling loss of the Si_3N_4 chip is measured to be about 4.5 dB/facet, while the fibre-to-fibre optical insertion loss is 10.3 dB. A PD is applied after the chip to down convert the signal to the electrical domain. A vector network analyzer (VNA) is employed to measure the RF bandpass response of this MPF link.

In Section III-A, we measure the optical transmission of the fabricated Si_3N_4 chip, and the FSR and bandwidth of each MRR are evaluated. Besides, we analyze the thermal-optical tuning characteristic of the MRRs. In Section III-B, we measure the RF response of the MPF based on this chip. Furthermore, we experimentally exhibit the reconfigurability of its center frequency and bandwidth.

A. The Measuring of the Fabricated Si_3N_4 Chip

We measure the transmission spectrum of the fabricated cascaded MRR filter pool chip through an advanced optical

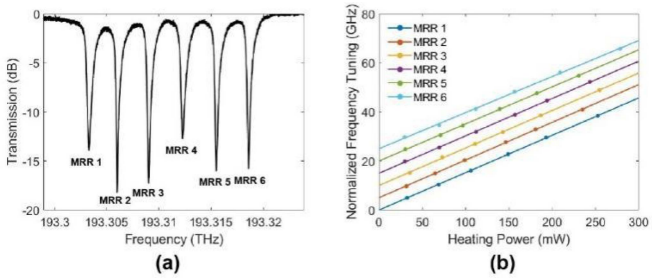

Fig. 5. (a) The optical transmission spectrum of the cascaded MRR notch filter. Thermal voltages are applied to divide the six MRRs and construct a uniformly distributed center wavelength. (b) The thermo-optical tuning characteristic of the chip.

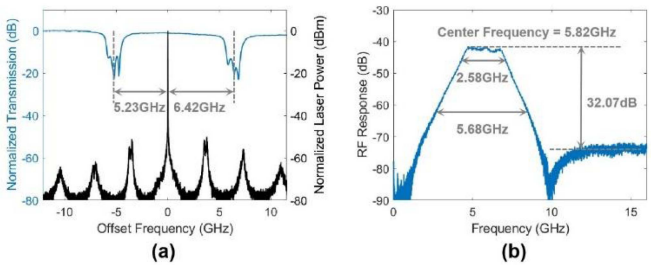

Fig. 6. (a) The normalized transmission spectrum of the cascaded MRR notch filter and the normalized laser spectrum. (b) The corresponding RF filtering response.

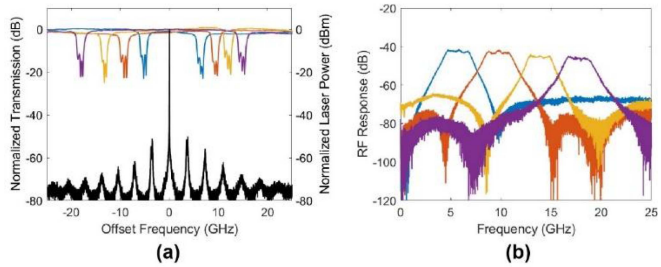

Fig. 7. (a) The optical spectrum of the notch filter in different working frequency. The spectrum of the laser source is shown with black line. (b) The corresponding RF filtering response tuning from 5.8 GHz to 18.2 GHz.

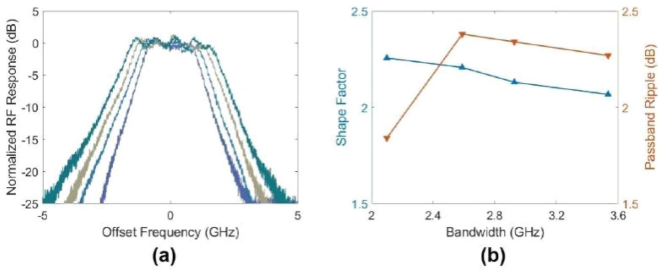

Fig. 8. (a) Bandwidth tuning of the MWP bandpass filter from 2.1 GHz to 3.5 GHz. (b) The shape factor and the passband ripple of the filtering spectrum in (a).

spectrum analyzer (OSA, APEX, AP2081B) with a built-in tunable laser, as shown in Fig. 5(a). The free spectrum ranges (FSRs) of all the MRRs are measured to be 260.8 GHz, and their bandwidths are 880 MHz. Besides, the extinction ratios of all the six MRRs are all below −13 dB. By applying voltage on the micro-heater, the temperature of the corresponding MRR increases, which leads to the change of the refractive index. In this way, the center frequency of the MRR is tuned. We measure the center frequencies of the six MRRs under increasing heating power through the monitor ports. The thermo-optical tuning characteristic of the MRRs are displayed in Fig. 5(b), and we observe a good linear correlation between the frequency tuning and heating power of about 0.15 GHz/mW. Meanwhile, each MRR shows an over 30 GHz tuning range with a heating power of up to 240 mW, which induces great flexibility to the notch spectrum of the chip.

B. System Performance

We establish the reconfigurable bandpass MPF with the cascaded MRR filter pool chip stated above. Firstly, we adjust the thermal tuning voltages on the six MRRs to meet the requirements of the center frequencies stated in (8), and the corresponding tuning powers are 50.9 mW, 28.2 mW, 4.8 mW, 68.7 mW, 39.2 mW, and 22.0 mW, respectively. The obtained normalized optical spectrum of the cascaded MRR filter pool and the normalized spectrum of the laser source are shown in Fig. 6(a). Here, the difference between the center frequency of the left notch filtering spectrum and the laser is 5.23 GHz, and the difference of the right one is 6.42 GHz. Besides, the separation between the center frequencies of MRRs is about 510 MHz. Hence, a RF bandpass response with a center frequency of 5.82 GHz is obtained as shown in Fig. 6(b). The 3-dB and 20-dB bandwidth of the RF response are 2.58 GHz and 5.68 GHz, respectively. Thus, the shape factor of the RF bandpass response is determined to be 2.2. Besides, the rejection ratio of the RF response is 32.07 dB.

We then evaluate the reconfigurability of the MPF system. We fix the Δf and change the f_0 of the optical filtering responses to evaluate the center frequency tunability of the proposed MPF. The obtained normalized optical spectrum is characterized in Fig. 7(a). Hence, the corresponding center frequency tuning within 5.8–18.2 GHz is shown in Fig. 7(b). The RF responses of the MPF at different center frequencies exhibit approximately the same bandwidth of ∼2.5 GHz and shape factors of ∼2.2.

On the other hand, the bandwidth reconfigurability of the MPF system is evaluated. By adjusting Δf of the optical filtering responses with fixed f_0, the 3-dB bandwidth of the RF response is demonstrated to be tunable from 2.1 GHz to 3.5 GHz, as shown in Fig. 8(a). The shape factors of the bandpass MPF responses are maintained around 2.2 with the bandwidth tuning, as shown in Fig. 8(b). Besides, the passband ripples of the RF responses are kept below 2.5 dB.

We investigate the RF link performance of the proposed MPF system with the method of two-tone test [33]. Two tone signals centered at different frequencies with a frequency interval of 20 MHz are generated by two synthesized signal generators. We feed the two-tone signal into the MPF system and measure the output powers of fundamental tones and intermodulation distortion (IMD) tones with different RF input powers. The measured RF gain, noise factor (NF) and SFDR are evaluated

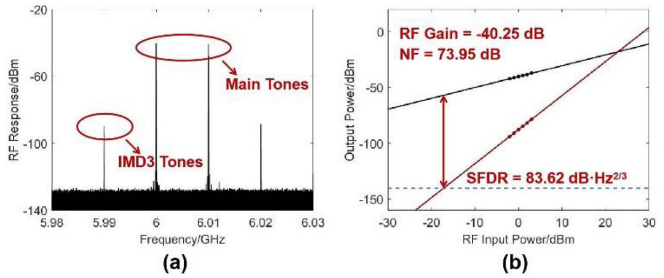

Fig. 9. (a) Measured RF spectrum after being processed by the proposed MPF system. (b) Measured RF Gain, NF and SFDR with the two-tone test signal centered at 6.005 GHz and the MPF centered at 6 GHz.

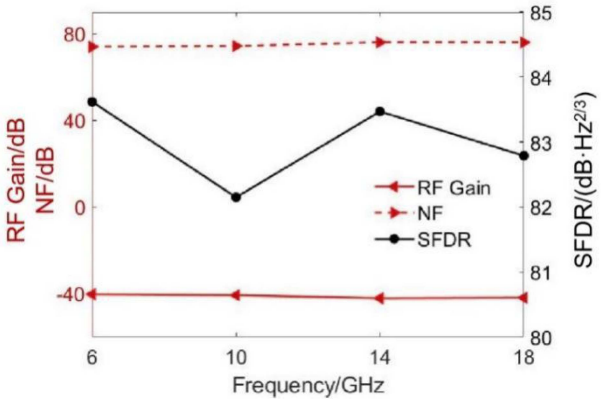

Fig. 10. RF Gain, NF and SFDR of the MPF system measured as functions at different frequency.

by fitting the measured powers and the input RF powers as functions, which are shown in Fig. 9(b).

Fig. 10 displays the RF Gain, NF and SFDR with the two-tone test signal centered at different frequencies. Within the center frequency tuning range (5.8–18.2 GHz), the proposed MPF system maintains good RF link performance: the RF Gain ranges from −42.13 dB to −40.25 dB, the NF ranges from 73.95 dB to 76.03 dB, and the SFDR ranges from 82.15 dB·Hz$^{2/3}$ to 83.62 dB·Hz$^{2/3}$.

Furthermore, we repeat the experiments stated above with only four of the six cascaded MRRs to evaluate the robustness of the MPF system, where the center frequencies of the other two MRRs are tuning 20 GHz away from the optical sideband. Here, by fixing the Δf and change the f_0 of the optical filtering responses, the center frequency of the proposed MPF can be tuned within 2.0 GHz–18.1 GHz, as shown in Fig. 11(b). In Fig. 11(a), we characterize the normalized optical spectrums of the applied four cascaded MRRs corresponding to the displayed RF responses in Fig. 11(b). The RF responses of the MPF at different center frequencies exhibit approximately the same bandwidth of ∼1.8 GHz and shape factors of ∼2.1. In this way, the tuning range of the bandwidth of the proposed MPF system could be further extended by changing the number of the cascaded MRRs, which demonstrates the scalability of the scheme. Besides, as mentioned before, the fibre-to-fibre optical insertion loss is 10.3 dB and the optical coupling loss is 9 dB, which indicates that the on-chip optical loss of the cascaded

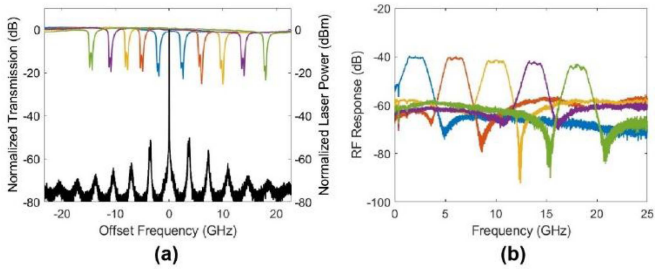

Fig. 11. (a) The optical spectrum of the notch filter in different working frequency in the case that four MRRs are cascaded to form the notch filter. The spectrum of the laser source is shown with black line. (b) The corresponding RF filtering response tuning from 2 GHz to 18 GHz.

MRRs is 1.3 dB, or an average of 0.2 dB per MRR. Therefore, the optical loss is barely irrelevant to the number of cascaded MRRs, and this scheme shows a potential to integrate more MRRs into the filter pool and achieve broader tuning bandwidth.

IV. Conclusion

In conclusion, we have demonstrated a reconfigurable RF bandpass filter with good shape factor based on a cascaded MRR filter pool on Si_3N_4 platform. The demonstrated microwave photonic filter system shows reconfigurabilities of both center frequency and bandwidth with a good shape factor of ∼2.2 and a high rejection ratio of ∼32 dB. The center frequency can be tuned from 5.8 GHz to 18.2 GHz and the bandwidth can be tuned from 2.1 GHz to 3.5 GHz. Comparing to the works based on cascaded MRRs before, we directly apply the combination of the optical notch spectrum to control the sidebands rather than introduce π phase shift. Therefore, our scheme provides an optimized passband ripple in broadband usage, which could reduce the distortion of RF signal. Moreover, with only part of MRRs in the working band, the proposed could offer a reduced bandwidth of ∼1.8 GHz for different RF applications. Besides, this scheme exhibits a significant potential for further extension. The proposed scheme is expected to play an important role in future broadband RF applications.

References

[1] A. D. Panagopoulos, P.-D. M. Arapoglou, and P. G. Cottis, "Satellite communications at KU, KA, and V bands: Propagation impairments and mitigation techniques," *IEEE Commun. Surveys Tuts.*, vol. 6, no. 3, pp. 2–14, Third Quarter 2004.

[2] C. T. Rodenbeck et al., "Ultra-wideband low-cost phased-array radars," *IEEE Trans. Microw. Theory Tech.*, vol. 53, no. 12, pp. 3697–3703, Dec. 2005.

[3] A. E. Spezio, "Electronic warfare systems," *IEEE Trans. Microw. Theory Tech.*, vol. 50, no. 3, pp. 633–644, Mar. 2002.

[4] W. J. Chappell, E. J. Naglich, C. Maxey, and A. C. Guyette, "Putting the radio in 'software-defined radio': Hardware developments for adaptable RF systems," *Proc. IEEE*, vol. 102, no. 3, pp. 307–320, Mar. 2014.

[5] R. G. Machado and A. M. Wyglinski, "Software-defined radio: Bridging the analog–digital divide," *Proc. IEEE*, vol. 103, no. 3, pp. 409–423, Mar. 2015.

[6] Y. Xu and P. R. Kinget, "A switched-capacitor RF front end with embedded programmable high-order filtering," *IEEE J. Solid-State Circuits*, vol. 51, no. 5, pp. 1154–1167, May 2016.

[7] S. Sabbagh and K. Mafinezhad, "4–6.3 GHz microwave tunable filter employing RF MEMS switches," in *Proc. 6th Int. Symp. Telecommun.*, 2012, pp. 37–41.

[8] D. Marpaung, C. Roeloffzen, R. Heideman, A. Leinse, S. Sales, and J. Capmany, "Integrated microwave photonics," *Laser Photon. Rev.*, vol. 7, pp. 506–538, 2013.
[9] J. Capmany and D. Novak, "Microwave photonics combines two worlds," *Nature Photon.*, vol. 1, no. 6, pp. 319–330, 2007.
[10] G. Serafino, S. Maresca, C. Porzi, F. Scotti, P. Ghelfi, and A. Bogoni, "Microwave photonics for remote sensing: From basic concepts to high-level functionalities," *J. Lightw. Technol.*, vol. 38, no. 19, pp. 5339–5355, Oct. 2020.
[11] Z. Jiao and J. Yao, "Passband-switchable and frequency-tunable dual-passband microwave photonic filter," *J. Lightw. Technol.*, vol. 38, no. 19, pp. 5333–5338, Oct. 2020.
[12] L. Yi et al., "Polarization-independent rectangular microwave photonic filter based on stimulated Brillouin scattering," *J. Lightw. Technol.*, vol. 34, no. 2, pp. 669–675, Jan. 2016.
[13] Y. Yanagase, S. Suzuki, Y. Kokubun, and S. T. Chu, "Box-like filter response and expansion of FSR by a vertically triple coupled microring resonator filter," *J. Lightw. Technol.*, vol. 20, no. 8, pp. 1525–1529, Aug. 2002.
[14] T. Kato and Y. Kokubun, "Bessel–Thompson filter using double-series-coupled microring resonator," *J. Lightw. Technol.*, vol. 26, no. 22, pp. 3694–3698, Nov. 2008.
[15] Z. Zhang, B. Huang, Z. Zhang, C. Cheng, and H. Chen, "Microwave photonic filter with reconfigurable and tunable bandpass response using integrated optical signal processor based on microring resonator," *Opt. Eng.*, vol. 52, no. 12, 2013, Art. no. 127102.
[16] Y. Liu et al., "Tunable and reconfigurable microwave photonic bandpass filter based on cascaded silicon microring resonators," *J. Lightw. Technol.*, vol. 40, no. 14, pp. 4655–4662, Jul. 2022.
[17] P. Alipour et al., "Fully reconfigurable compact RF photonic filters using high-Q silicon microdisk resonators," *Opt. Exp.*, vol. 19, pp. 15899–15907, 2011.
[18] A. M. Gutierrez et al., "Ring-assisted Mach–Zehnder interferometer silicon modulator for enhanced performance," *J. Lightw. Technol.*, vol. 30, no. 1, pp. 9–14, Jan. 2012.
[19] N. Kohli, B. L. Sang, F. Nabki, and M. Ménard, "Tunable bandpass filter with serially coupled ring resonators assisted MZI," *IEEE Photon. J.*, vol. 13, no. 4, Aug. 2021, Art. no. 6600608.
[20] S. S. Djordjevic et al., "Fully reconfigurable silicon photonic lattice filters with four cascaded unit cells," *IEEE Photon. Technol. Lett.*, vol. 23, no. 1, pp. 42–44, Jan. 2011.
[21] M. T. Boroojerdi, M. Ménard, and A. G. Kirk, "Wavelength tunable integrated add-drop filter with 10.6 nm bandwidth adjustability," *Opt. Exp.*, vol. 24, no. 19, pp. 22043–22050, 2016.
[22] J. Palaci, G. E. Villanueva, J. V. Galán, J. Marti, and B. Vidal, "Single bandpass photonic microwave filter based on a notch ring resonator," *IEEE Photon. Technol. Lett.*, vol. 22, no. 17, pp. 1276–1278, Sep. 2010.
[23] G. Brunetti, F. Dell'Olio, D. Conteduca, M. N. Armenise, and C. Ciminelli, "Ultra-compact tuneable notch filter using silicon photonic crystal ring resonator," *J. Lightw. Technol.*, vol. 37, no. 13, pp. 2970–2980, Jul. 2019.
[24] H. Shen et al., "Eight-channel reconfigurable microring filters with tunable frequency, extinction ratio and bandwidth," *Opt. Exp.*, vol. 18, pp. 18067–18076, 2010.
[25] L. Liu, M. He, and J. Dong, "Compact continuously tunable microwave photonic filters based on cascaded silicon microring resonators," *Opt. Commun.*, vol. 363, pp. 128–133, 2016.
[26] Y. London et al., "Performance requirements for terabit-class silicon photonic links based on cascaded microring resonators," *J. Lightw. Technol.*, vol. 38, no. 13, pp. 3469–3477, Jul. 2020.
[27] H. Jiang, L. Yan, and D. Marpaung, "Chip-based arbitrary radio-frequency photonic filter with algorithm-driven reconfigurable resolution," *Opt. Lett.*, vol. 43, no. 3, pp. 415–418, 2018.
[28] O. Daulay, R. Botter, and D. Marpaung, "On-chip programmable microwave photonic filter with an integrated optical carrier processor," *Opt. Soc. Amer. Continuum*, vol. 3, no. 8, pp. 2166–2174, 2020.
[29] Y. Chen, Z. Fan, Y. Lin, D. Jiang, X. Li, and Q. Qiu, "A multiband microwave photonic filter based on a strongly coupled microring resonator with adjustable bandwidth," *IEEE Photon. J.*, vol. 15, no. 1, Feb. 2023, Art. no. 5500206.
[30] Y. Stern et al., "Tunable sharp and highly selective microwave-photonic band-pass filters based on stimulated Brillouin scattering," *Photon. Res.*, vol. 2, pp. B18–B25, 2014.
[31] S. Song, S. X. Chew, X. Yi, L. Nguyen, and R. A. Minasian, "Tunable single-passband microwave photonic filter based on integrated optical double notch filter," *J. Lightw. Technol.*, vol. 36, no. 19, pp. 4557–4564, Oct. 2018.
[32] J. Li, S. Yang, H. Chen, and M. Chen, "Subwavelength hole defect assisted microring resonator for a compact rectangular filter," *Opt. Lett.*, vol. 45, pp. 3123–3126, 2020.
[33] J. Li, S. Yang, H. Chen, and M. Chen, "Hybrid microwave photonic receiver based on integrated tunable bandpass filters," *Opt. Exp.*, vol. 29, no. 7, pp. 11084–11093, 2021.